The Bouncing Ball Apparatus as an Experimental Tool

Ananth Kini
Aerospace and Mechanical Engineering, University of Arizona
Tucson, AZ 85721, USA

Thomas L. Vincent
Aerospace and Mechanical Engineering, University of Arizona
Tucson, AZ 85721, USA

Brad Paden
Mechanical and Environmental Engineering, University of California,
Santa Barbara, CA 93106, USA.

Abstract

The bouncing ball apparatus exhibits a rich variety of nonlinear dynamical behavior and is one of the simplest mechanical systems to produce chaotic behavior. A computer control system is designed for output calibration, state determination, system identification and control of the bouncing ball apparatus designed by Launch Point Technologies. Two experimental methods are used to determine the co-efficient of restitution of the ball, an extremely sensitive parameter of the apparatus. The first method uses data directly from a stable 1-cycle orbit. The second method is based on the ball map combined with data from a stable 1-cycle orbit. For control purposes, two methods are used to construct linear maps. The first map is determined by collecting data directly from the apparatus. The second map is determined from linearization of the ball map. The maps are used to estimate the domains of attraction to the stable 1-cycle orbit. These domains of attraction are used with a chaotic control algorithm to control the ball to a stable 1-cycle, from any initial state. Results are compared and it is found that the linear map obtained directly from the data gives the more accurate representation of the domain of attraction.

1 Introduction

The bouncing ball system consists of a ball bouncing on a plate whose amplitude is fixed and the frequency of vibration is controlled. The plate is driven using a sinusoidal control signal. The bouncing ball system exhibits a rich variety of nonlinear dynamical behavior. It is one of the simplest deterministic physical systems to exhibit chaotic motion. A complete theoretical study of a ball bouncing on a vibrating plate has been given in [1]. It has been demonstrated that depending on the initial conditions of the ball and the frequency at which the plate is driven, the ball can exhibit chaotic or periodic motion. For example, the ball can undergo an n-cycle periodic motion corresponding to certain frequencies. A simple 1-cycle periodic motion is such that the ball bounces to a constant height and after each bounce, the plate undergoes one complete cycle before the next bounce. Similarly, the plate could complete n-cycles (the value of n depending upon the frequency of vibration of the plate) as the ball bounces to a constant height. The bounce heights increase with increasing value of n. The ball can also bounce to m different heights for every n cycles of the plate. Chaotic motion is observed at certain driving frequencies of the plate. It is shown in [1] that a ball map for the bouncing ball system is a ‘Smale horseshoe’, which is an indicator that the motion of the ball is chaotic at certain frequencies.

The bouncing ball is extremely sensitive to the parameters that define the system and these need to be determined accurately for modeling and control purposes. We will demonstrate how stable periodic motion can be used to determine the parameters for the experimental system described in section 1.1. A high-bounce map can be used to represent the experimental system, when the amplitude of the piston is small compared to the height to which the ball bounces, as demonstrated in [2]. We use a high-bounce

map to model the experimental system, and using experimental data along with equilibrium solutions to the high-bounce map, determine the parameters of the experimental system. These are used to construct a mathematical model of the bouncing ball experimental system.

This model is used to construct a linear map of the system about a fixed point corresponding to one of the stable 1-cycle periodic frequencies by linearization of the high-bounce map [3]. Alternately, experimentally determined parameters along with a data-based approximation method [3, 4] is used to construct a linear map of the bouncing ball system about the same fixed point. These two linear maps are used to design controllers to the fixed point.

A chaotic control algorithm [5] is used to drive the ball to the fixed point. Estimates of the domain of attraction to the fixed point, essential for this algorithm, are obtained using the two linear maps mentioned earlier. Controllers are designed using these domains of attraction. They drive the ball to the fixed point and the effectiveness of using the two linear maps to represent the experimental system is compared using data collected from the experiment.

1.1 Description of the Apparatus

The bouncing ball apparatus (BBA) is an experimental system manufactured by Launch Point Technologies [www.launchpt.com] and is illustrated in Figure 1. This design is based on a laboratory system used in previous studies [2, 4]. The plate, in this case is a piston, and is driven by a voice coil type actuator having a stroke limited by rubber bumpers. An external command input (typically a sinusoidal waveform) is supplied as a reference to control the motion of the piston. A "super ball", is confined to bounce along a tensioned stainless steel rod. The ball has an internal Teflon bushing to allow it to move smoothly along the stainless steel rod and friction does not play a major role with the BBA. Moreover, the rod is lubricated with a light spray lubricant. Friction is not considered to be present while modeling the motion of the ball.

The position of the piston is measured using an inductance coil etched on the printed circuit board. The inductance of this coil changes as a tapered section of the aluminum piston assembly moves through the coil and is detected using a crystal-controlled coherently-demodulated sensing scheme. This is fed back through a high-bandwidth PD controller and is used to control the amplitude and frequency of the piston according to the externally supplied reference control input. This internal control system loop for maintaining the reference input is depicted in Figure 2. Ideally, the motion of the piston should be unaffected by the impacts with the ball. The internal controller for the piston approximates this situation and the piston, though affected by the impact, recovers quickly. A ball-bounce sensor consists of a microphone in the piston and is in acoustic communication with the ball impact surface via an acoustic waveguide. The channel inlet is on the top of the piston. The output from the microphone is an analog signal and this can be used to compute the time of bounce. The signals from the piston position sensor and the microphone are provided as outputs and are used to compute the state of the system. The reference input may be provided using a signal generator (open loop) or a closed-loop computer control system (by adding an outer control loop). Our interest here is in designing an outer control loop in order to obtain the desired stable periodic motion.

(a) (b)

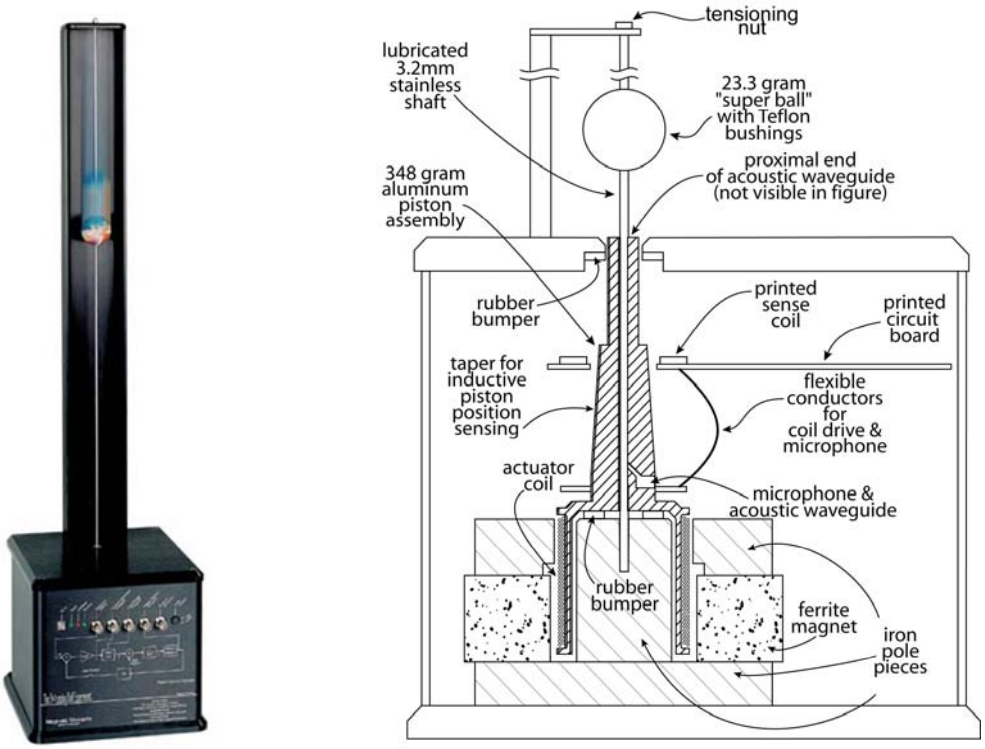

Figure 1: (a) Photograph of the bouncing ball apparatus (BBA) (b) A front section drawing of the BBA BBA has 5 external connections: 1. Reference (input) 2. Current Command (output) 3. Coil Voltage (output) 4. Piston Position (output) 5. Bounce (output)

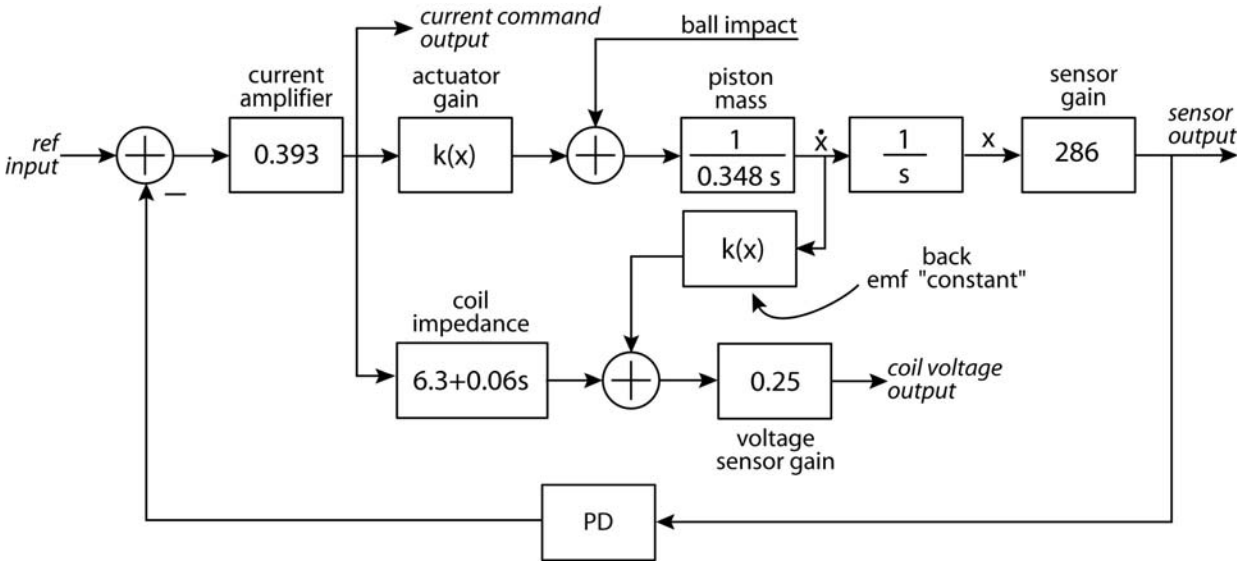

Figure 2: Internal control system loop in the BBA

1.2 Interfacing the BBA with a computer

The outer control loop consists of a computer control system using a data acquisition card to acquire the output signals from the BBA and to supply the control signal as a reference input to the BBA, as shown in Figure 3.

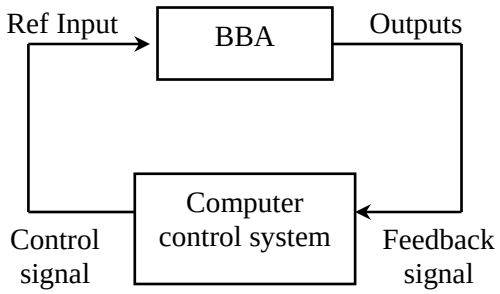

Figure 3: Outer computer control system loop for BBA

The computer control system computes the state of the system based on the output from BBA. This is then used to generate a control signal to the experimental system based on any chosen control algorithm. The output from the piston position sensor is a voltage and this is calibrated in terms of a displacement of the piston in meters with respect to the position of the piston when no control input is supplied. The microphone output is an analog signal that shows a spike when a bounce occurs. A variation of a zero crossing technique is used to identify the time of bounce. A pseudo-derivative filter is designed to estimate the velocity of the piston from the position signal. A combination of the piston position and velocity is used to compute the phase of the piston at bounce, which is one of the state variables of the BBA. The time between bounces, obtained from the microphone, along with the driving frequency of the plate is used to compute the phase change of the plate between bounces and this is the other state variable of the BBA.

1.3 Chaotic control algorithm

A number of control algorithms have been proposed to obtain various types of stable periodic motion. A frequency modulation technique has been used in [6] to achieve a 2-period motion or a stable periodic motion involving two bounces per period. The plate is driven at a certain base frequency and the instantaneous frequency is modulated to obtain arbitrary controlled bounce heights in 2-period motion. A chaotic control algorithm [2,5] has been used to control the ball to a stable 1-cycle periodic orbit starting from rest on the plate and has been implemented in simulation in [3]. It has been demonstrated to work on a laboratory system [4].

The chaotic control algorithm may be used to control the ball to any given stable or unstable periodic orbit. It uses a linear map to estimate the domain of attraction corresponding to a closed loop control law. The plate is initially driven chaotically using an open-loop sinusoidal input. The ball is driven chaotically until it enters the domain of attraction, corresponding to the closed-loop control law. The control is then switched to the closed-loop control to drive the ball to the fixed point.

We will consider here the simplest case of a stable n=1 orbit. In this case, we only have to switch the driving frequency to the frequency corresponding to the stable fixed orbits once the system enters the domain of attraction.

The key step in the implementation of this algorithm is to accurately estimate the domain of attraction. Two methods are used. In the first case, the linear map from the data-based approximation method is used to estimate the domain of attraction. In the second case, the domain of attraction is estimated using the linearized high-bounce map. In both cases, the ball is controlled to a fixed point corresponding to one of the stable 1-cycle periodic frequencies. Data is collected directly from the experiment and the trajectory of the ball is plotted. The effectiveness of these maps to represent the actual bouncing ball experimental system is compared.

2 Description of computer control system for BBA

A laptop computer is used to acquire and send signals to the bouncing ball experiment. A Simulink® model running on the laptop computer is used to design the outer computer control system loop. Real-Time Windows Target® is the real-time kernel used to interface the bouncing ball system with the Simulink® model executing on the computer. This real-time kernel running at CPU ring zero (privileged or kernel mode) ensures that the applications run in real-time using the built in PC clock as its primary source of time. The Windows operating system running in the background does not disturb the real-time processes because the real-time kernel intercepts the interrupts from the PC clock before it goes to the Windows operating system. It then uses the interrupts to trigger the execution of the compiled Simulink® model, thus giving the application the highest priority.

The Simulink® model is first converted into C code and an executable specific to the Real-Time Windows Target® by using Real-Time Workshop® and downloaded on to the real-time kernel. It then runs in this environment interacting with the external system and carrying out the various data acquisition and control tasks. The Simulink® model acts like a user-interface allowing the user to change parameters and view target signals while the code is executing in the kernel. This feature can be used for online parameter tuning and signal monitoring

Figure 4 shows how a Simulink® model running on the computer interacts with the bouncing ball experiment via the Real-Time Windows Target® interface. In our case, the model executes on a Laptop PC, which has a National Instruments® DAQCard-6062E I/O board that takes in feedback data from the experiment and then sends a control output as an analog voltage to the power amplifier. The power amplifier then sends a current input to the voice coil actuator, which in turn is used to position the piston. The connector block is used to make the physical wire connections for the Daqcard-6062E. The outputs from the BBA that are fed back to the computer are the current command output from the power amplifier, the coil voltage from the voice coil actuator, the piston position as a voltage from the piston position sensor and the bounce output as an analog voltage signal from a microphone.

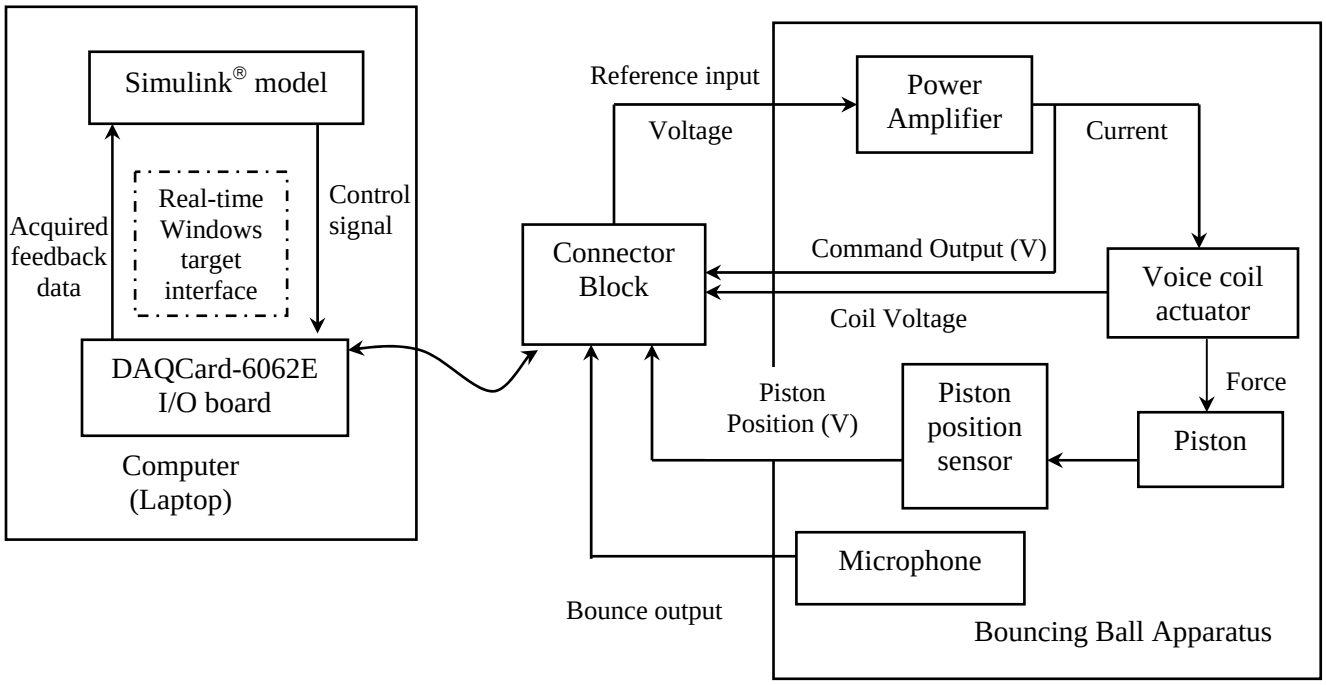

Figure 4: Schematic of the laboratory set-up for the bouncing ball experiment

3 Calibration and state determination

A number of characteristics of the BBA need to be determined before a control system can be designed. These include the linear relation between the reference input voltage and the piston displacement, and the phase characteristics of the piston motion with respect to the control voltage signal. Also, the outputs of the actuators and the sensors, provided by the BBA have to be calibrated, which are then used in the estimation of the state of the system. All measurements are carried out using the computer control system described in the previous section.

3.1 Calibration of the piston position sensor

The piston position sensor is calibrated in order to obtain the corresponding displacement of the piston in meters. The position of the piston is to be determined as a displacement from its zero position, corresponding to a zero reference input signal. The piston displacements for various values of the reference input voltages are measured using a height gauge. The displacement of the piston versus the piston position sensor output is plotted in Figure 5. The variation is nearly linear and is represented by the straight-line equation

$$Y = -0.003X_o,$$

where Y is the piston position measured in meters with respect to the zero position and X_o is the output voltage in (V)

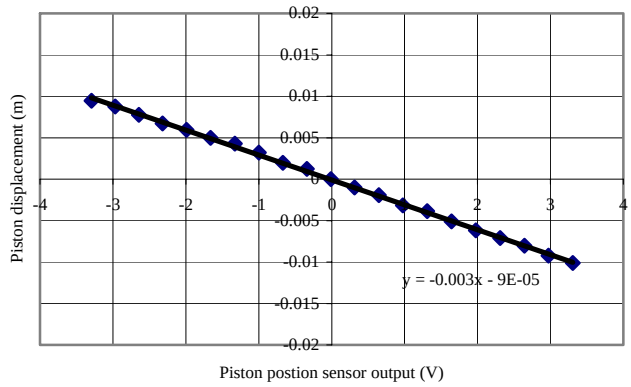

Figure 5: Piston position sensor calibration plot

3.2 Linearity and frequency response of piston

A voltage signal is applied a reference input to the BBA to control the piston position. The internal piston control system is kept closed. The piston displacement is observed to be linear with respect to the input signal and is represented by the equation

$$Y = -0.001X_i ,$$

where Y is the piston position measured in meters and X_i is the reference input voltage in volts.

The frequency response of the piston [7] is obtained by supplying a sinusoidal reference input signal to the BBA at different frequencies. The amplitudes of the reference input signal and the output signal from the piston position sensor, and the phase difference between the two is measured at these frequencies and is plotted in Figure 6. The dashed line indicates the trend of the piston margin plot. A cutoff frequency of 110 Hz was obtained as shown by the dotted line. The phase plot indicates that there is no significant difference between the input and output signals for frequencies up to about 50 rad/s which and can be ignored for all practical purposes.

(a) (b)

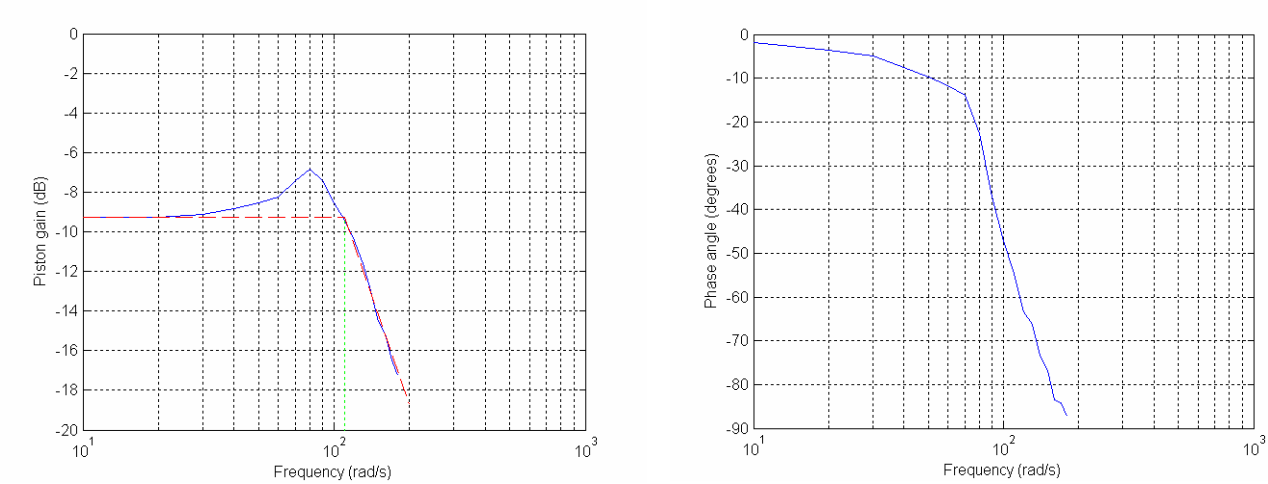

Figure 6: frequency response of piston - a) Piston gain characteristics b) Piston phase characteristics

3.3 Bounce detection using microphone, data acquisition system

A ball-bounce sensor is provided in the BBA to detect the collision between the piston and the ball. This uses a microphone to record the sound of collision. This signal from the microphone is amplified and filtered and is then provided as the bounce output of the BBA. This analog signal is read through the data acquisition card into the laptop computer and the computer control system described earlier. The bounce times are extracted by using a modified zero-crossing detection technique.

The bounce output signal for a 1-cycle periodic bounce is shown in Figure 7. (a). The bounce output is an analog signal undergoing oscillations about a certain value (due to the piston motion) when no bounce has occurred. When a bounce occurs there is a spike in the oscillation in the negative direction. The bounce output has been magnified to show two consecutive pulses in Figure 7. (b). A closer look at the pulse shows that the peak pulse at each bounce undergoes an oscillation. The signal crosses the zero from the positive and the negative sides twice. The time of bounce is given by the time at which the signal first crosses the zero axis. A direct zero crossing technique based on a falling edge cannot be applied as this would lead to triggering of false bounces. In order to avoid this, some logic has to be incorporated to capture just the first falling edge.

It is observed that the second falling edge occurs within 10ms of the first falling edge. The time between consecutive bounces is greater than this (order of 180-300ms). So, a falling edge is considered as a bounce only if a falling edge has not occurred within the previous 10ms. This is implemented by recording the zero crossing time at which the falling edge occurs and then comparing this value with the zero crossing time of the previous falling edge that has been stored in memory. If this value is greater than 10ms, then a bounce is said to have occurred. The corresponding time of bounce and the piston position are recorded. The time between bounces can be obtained from this.

(a) (b)

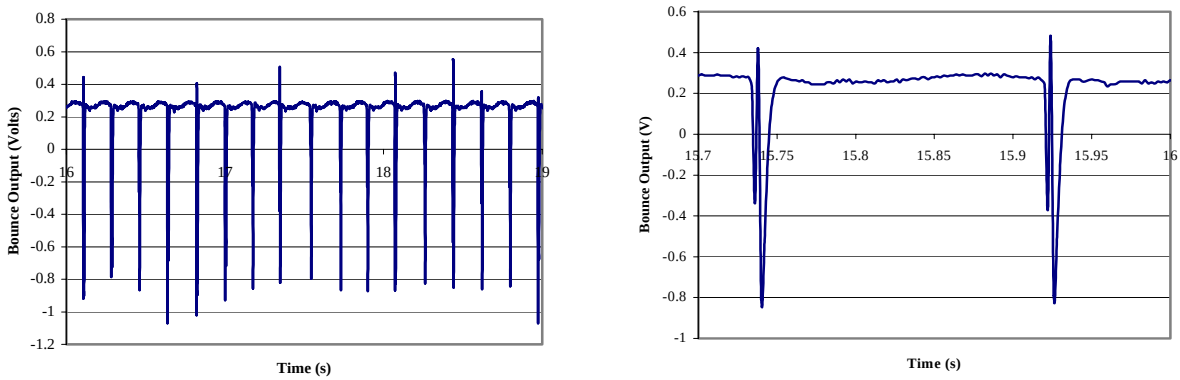

Figure 7: (a) Bounce Output signal recorder for a 1-cycle periodic bounce (b) The Bounce output signal magnified to show two consecutive pulses

3.4 Pseudo-derivative filter for velocity estimation

The velocity of the piston at the time of bounce is needed to compute the phase of the piston, from the position signal. The sign of position and the velocity are used to estimate in which quadrant the phase angle lies. The velocity is estimated from the position signal using a pseudo-derivative filter [8].

The transfer function of the pseudo-derivative filter is given by:

$$G_{pd}(s) = \frac{y(s)}{u(s)} = \frac{s}{1+\varepsilon s} \quad , \qquad (0.1)$$

where $\varepsilon = 1/f_{pd}$, f_{pd} denotes the pseudo-derivative cut-off frequency. This filter differentiates over the frequency range $0 < \omega < f_{pd}$ (ω is the frequency of the position signal. f_{pd} was obtained earlier in figure 6 as 110 rad/s and represents the maximum frequency of the position signal expected.

$$\varepsilon = \frac{1}{110} = 0.00909$$

This filter is converted to discrete form in order to apply it to the discrete time position signal obtained into computer through the data acquisitions system. In order to discretize (0.1), a mapping from the s-plane to the z-plane is obtained using the Tustin's method.

$$s = \frac{2}{T}\frac{1-z^{-1}}{1+z^{-1}} \quad ,$$

where T = sampling time for the input position signal.

The discretized state space equivalent of (0.1) is written as:

$$\begin{aligned} x(t+1) &= Ax(t) + Bu(t) \\ y(t) &= Cx(t) + Du(t) \quad , \end{aligned} \tag{0.3}$$

where A = 0.8018, B = 0.9009, C = -21.8018, D = 99.0991 with a T = 0.002s.

A Bode plot of the continuous and discrete-time pseudo-derivative filters, shown in Figure 8: (a), demonstrates that the discrete time filter is a good approximation of the continuous filter over the frequency range 0-200 rad/s. The implementation of the discrete pseudo-derivative filter within a Simulink® model is shown in Figure 8: (b)

(a)

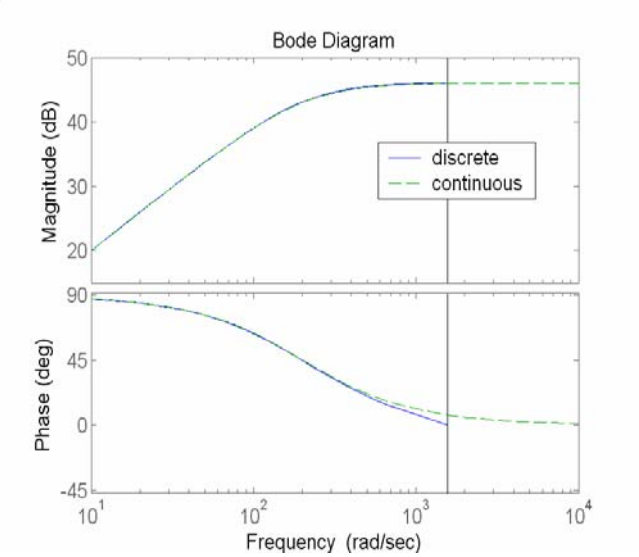

(b)

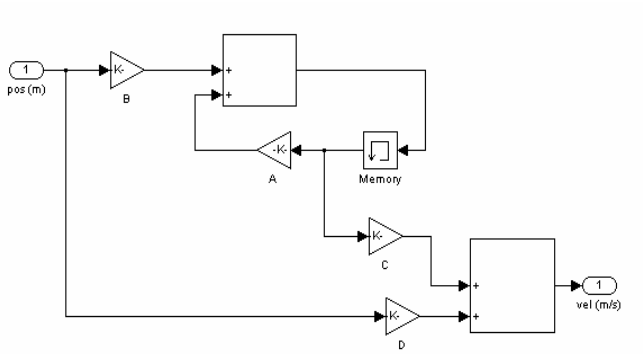

Figure 8: (a) Bode Plots of the continuous and discrete-time pseudo-derivative filters (b) Simulink® block implementation of the discrete-time pseudo derivative filter for velocity estimation

4 System identification

The state variables for the BBA are the mass ratio (M) and the co-efficient of restitution of the ball (e). The mass ratio is defined as the ratio of the mass of the ball to the mass of the piston. This is known accurately from direct measurement. The co-efficient of restitution is defined as the ratio of the relative velocities of ball and piston before and after collision. This parameter must be determined indirectly.

Two different methods are employed to determine 'e' of the ball in the BBA. The first method uses the definition of 'e' and the data collected from the BBA by putting the ball into a stable periodic orbit. The second method uses the data collected from the BBA and the periodic solutions to the high-bounce map used to represent the BBA. The methods used in the determination of the parameters will give insights into the rich nonlinear dynamics of the bouncing ball apparatus.

Using the value of ‘e’ from the first method and data obtained experimentally, a linear map of the BBA is estimated. A second linear map for the BBA is constructed using the value of ‘e’ from the second method and a direct linearization of the high bounce map. A comparison of the two linear maps is made.

4.1 Co-efficient of restitution

The co-efficient of restitution (e) is an extremely sensitive parameter of the system. It is written in terms of the known parameters of the system. Let U_j and V_j be the upward velocities of the piston just before and after the last bounce, and let W_j and W_j’ be the upward velocities of the piston just before and just after. Using the definition of ‘e’,

$$V_j - W_j' = -e(U_j - W_j), \tag{1}$$

where the negative sign comes from the reversal of directions of relative velocities. By the Conservation of momentum,

$$W_j + MU_j = W_j' + MV_j. \tag{2}$$

Eliminating W_j’ between (1) and (2) gives,

$$e = \frac{(1+M)V_j - MU_j - W_j}{W_j - U_j}. \tag{4}$$

Removing the ball from the apparatus and measuring the bounce heights by dropping the ball on a rigid surface from a known height cannot be used to determine the value of ‘e’. This is because the presence of the shaft through the ball does not yield consistent results. The procedure of dropping the ball on the stationary rigid surface from an arbitrary height and recording the time between bounces is suggested in [9]. This procedure was tried by bouncing the ball on the BBA piston with a constant voltage input to hold the piston stationary. The value of ‘e’ was estimated to be 0.713. However, this is not an accurate value of ‘e’ for the ball. The reason for this is that, ideally, the piston should have an infinite mass so that its motion is unaffected by the impacts with the ball. The controller for the piston only approximates this situation. The piston undergoes small oscillations on impact with the ball and does not act like a perfectly rigid surface. The ball map is extremely sensitive to the value of ‘e’ and hence it must be determined by some other method. A unique procedure that takes advantage of the dynamics of the systems is proposed to determine the value of ‘e’ in the next section.

4.2 Determination of the co-efficient of restitution using experimental data

The definition of ‘e’ and the data collected by putting the ball into a stable 1-cycle periodic motion will be used to determine ‘e’. For stable 1-cycle periodic motion, the ball bounces to a constant height. In this case, the magnitude of the velocities U_j and V_j will be equal with the directions being opposite for every bounce,

$$U_j = -V_j. \tag{5}$$

Substituting for U_j from (5) in (4) we get,

$$e = \frac{(1+2M)V_j - W_j}{W_j + V_j}. \tag{6}$$

The motion of the piston is controlled according to

$$y = A\sin(\omega_j \tau + \phi_j), \tag{7}$$

where y is the vertical displacement of the piston. The amplitude of oscillation of the piston is A, the frequency at the time of bounce is ω_j and $\tau = t - t_j$, is the time since the last bounce. The phase angle of the piston at the last bounce is given by ϕ_j.

$$\phi_j = \omega_j(t_j - t_{j-1}) + \phi_{j-1}, \tag{7.1}$$

The velocity of the piston is obtained by differentiating (7) to give

$$W(t) = A\omega_j \cos(\omega_j \tau + \phi_j). \tag{8}$$

Using the equation (5), the time between bounces can be written as

$$t_{j+1} - t_j = \frac{2V_j}{g}, \tag{9}$$

where t_j is the time at which the jth bounce occurs. The velocity V_j can be computed knowing the bounce times. Thus, by computing the value of W_j from equation (7) at the jth bounce and the velocity V_j from equation (8), we can compute the value of the co-efficient of restitution.

In order to obtain the value of e, we first put the ball into a stable 1-cycle periodic motion. An approximate range of frequencies at which stable 1-cycle periodic motion occurs can be determined by assuming a reasonable value of e, and then using frequencies close to this. In order to place the ball into a periodic orbit the ball has to be dropped from the initial height corresponding to the stable orbit and the piston must be in the proper position when the ball hits it. Since this is not known beforehand, trial and error is required.

The piston is supplied with a sinusoidal reference input of amplitude 0.008m at one of the approximate frequencies corresponding to 1-cycle periodic motion. The ball is dropped from an arbitrary height until it gets into a 1-cycle periodic orbit. The bounce times are noted for a number of bounces and these are used to compute the time between bounces and the phase of piston at the bounces.
Table 1 shows the mean value of the value of the phase of the piston at bounces, the time between bounces and the e value corresponding to a particular frequency. The data is collected using a Simulink® model using a Real-Time Windows Target® interface. This is repeated for a number of frequencies in order to average out the uncertainties in measurement and the slight variation of e at the different frequencies.

Frequency (rad/s)	Phase of piston at bounce - ϕ_j	Time between bounces - $t_{j+1} - t_j$ (s)	Co-efficient of restitution – e
27	25.32°	0.232	0.8276
29	37.16°	0.217	0.8218
31	44.86°	0.203	0.8185
33	50.83°	0.190	0.8162
35	56.23°	0.180	0.8236

Table 1: The e values, and the ϕ_j and ($t_{j+1} - t_j$) values at different frequencies corresponding to stable 1-cyle periodic orbits

The mean value of e is obtained to be **0.822.**

4.3 Linear map from experimental data

We construct a linear map for the BBA about a stable fixed point using data collected directly from the experiment. A small perturbation is applied to the frequency of vibration of the piston about one of the periodic orbits and data is collected from the apparatus. A least square analysis is carried out on the data to construct a linear map for the apparatus corresponding to a particular frequency as in [3].

The ball is first placed into a stable periodic orbit at a certain frequency input ($\overline{\omega}$). The mean values of the state variables of the system, namely, piston phase at bounce ϕ_j (= $\overline{\phi}$) and the phase change between the bounces ψ_j (= $\overline{\psi}$), are obtained from the system. This is done by taking the average of these values for a number of bounces at a particular stable periodic frequency. The piston is now driven at a slightly perturbed frequency ω. The values of ϕ_j and ψ_j are collected for (n+1) bounces starting from the kth bounce. This is collected for a large number of bounces in order to get an accurate representation of the system. The state variables

$$x_1 = \phi_j - \overline{\phi} \qquad (9.1)$$
$$x_2 = \psi_j - \overline{\psi},$$

are constructed by considering ϕ_j and ψ_j as perturbations in the nominal values of $\overline{\phi}$ and $\overline{\psi}$, and let

$$u = \omega - \overline{\omega} \qquad (9.2)$$

be a perturbation in the frequency from the nominal value $\overline{\omega}$. These state variables are computed for each bounce and a matrix Y is formulated to obtain

$$Y = \begin{bmatrix} x_{1_k} & x_{1_{k+1}} & x_{1_{k+2}} & \dots & x_{1_{k+n}} \\ x_{2_k} & x_{2_{k+1}} & x_{2_{k+2}} & \dots & x_{1_{k+n}} \end{bmatrix},$$

where the subscript represents the bounce number.

From this we can formulate the 2n x 1 vector

$$z = \begin{bmatrix} x_{1_{k+1}} \\ x^{1}_{2_{k+1}} \\ x_{1_{k+2}} \\ x_{2_{k+2}} \\ \vdots \\ x_{1_{k+n}} \\ x_{2_{k+n}} \end{bmatrix},$$

and the 2n x 6 matrix,

$$W = \begin{bmatrix} u & x_{1_k} & x_{2_k} & 0 & 0 & 0 \\ 0 & 0 & 0 & u & x_{1_k} & x_{2_k} \\ u & x_{1_{k+1`}} & x_{2_{k+1}} & 0 & 0 & 0 \\ 0 & 0 & 0 & u & x_{1_{k+1`}} & x_{2_{k+1}} \\ \vdots & \vdots & \vdots & \vdots & \vdots & \vdots \\ u & x_{1_{k+n-1}} & x_{2_{k+n-1}} & 0 & 0 & 0 \\ 0 & 0 & 0 & u & x_{1_{k+n-1}} & x_{2_{k+n-1}} \end{bmatrix}.$$

We then find the least squares solution to the equation

$$Wp = z$$

where

$$p = \begin{bmatrix} b_1 \\ a_{11} \\ a_{12} \\ b_2 \\ a_{21} \\ a_{22} \end{bmatrix}$$

Once p is determined, we can construct the linear map of the bouncing ball experimental system as

$$x_{j+1} = Ax_j + bu_j,$$

where

$$A = \begin{bmatrix} a_{11} & a_{12} \\ a_{21} & a_{22} \end{bmatrix} \text{ and } b = \begin{bmatrix} b_1 \\ b_2 \end{bmatrix}.$$

Using $\overline{\omega}$ = 30 rad/s and a perturbed frequency of ω =30.1 rad/s, we obtain

$$A = \begin{bmatrix} -0.5708 & 0.5111 \\ -1.6194 & 0.5201 \end{bmatrix} \text{ and } b = \begin{bmatrix} 0.2199 \\ 0.2146 \end{bmatrix}.$$

The eigenvalues of the A matrix are

$$\lambda = -0.0254 \pm 0.7281i \quad (|\lambda| = 0.729),$$

verifying that $\overline{\omega}$ is a stable orbit.

5 High-bounce map to represent BBA

We also estimate the parameters of the BBA, using a high-bounce map [1] to represent it. These parameters are then used to compute the parameters of the map. The high-bounce map is linearized and is compared to the data-based linear map obtained directly from data collected from the BBA. This is used to see if the high-bounce ball map is a good representation of the BBA and whether we can design controllers for the actual experimental system using this map.

In constructing the high-bounce map, we make a few assumptions so as to obtain a simple representation of the bouncing ball system as in [3]. We do not consider the presence of "uncertain" forces that are introduced due to the rod used to restrain the motion of the ball along a vertical and the air resistance. We also assume that the amplitude A of the piston is negligible compared with the height of the bounce.

The phase angle for the next bounce can be written using (7.1) as,

$$\phi_{j+1} = \omega_j (t_{j+1} - t_j) + \phi_j . \tag{10}$$

Rewriting (4) for V_j we get,

$$V_j = \left(\frac{M-e}{1+M}\right) U_j + \left(\frac{1+e}{1+M}\right) W_j , \tag{11}$$

$$\text{Define } a_1 = \left(\frac{M-e}{1+M}\right) \text{ and } a_2 = \left(\frac{1+e}{1+M}\right),$$

and evaluate V at the time of the next bounce, to obtain

$$V_{j+1} = a_2 U_{j+1} + a_1 W_{j+1} . \tag{12}$$

Using (8) velocity of the piston for the next bounce can be written as,

$$W_{j+1} = A\omega_j \cos(\omega_j (t_{j+1} - t_j) + \phi_j)$$

$$= A\omega_j \cos\phi_{j+1} \tag{13}$$

If we make the high-bounce approximation that the amplitude A is negligible compared with the height of the bounce, we can obtain explicit equations for the map. The high-bounce approximation gives

$$\begin{aligned} U_{j+1} &= -V_j \\ t_{j+1} - t_j &= \frac{2V_j}{g}, \end{aligned} \tag{14}$$

where g is the acceleration due to gravity.

It follows that (10) and (12) may be written as

$$\begin{aligned} \phi_{j+1} &= \omega_j\left(\frac{2V_j}{g}\right) + \phi_j \\ V_{j+1} &= -a_2 V_j + a_1 A\omega_j \cos\phi_{j+1} \end{aligned}$$

Multiply the last equation through by $2\overline{\omega}/g$ to give,

$$\frac{2\overline{\omega}}{g}V_{j+1} = -a_2\frac{2\overline{\omega}}{g}V_j + a_1 A\frac{2\overline{\omega}\omega_j}{g}\cos\phi_{j+1},$$

and define the phase angle change that takes place between the last bounce of the ball and the next as,

$$\psi_j = \frac{2\overline{\omega}V_j}{g}$$

we obtain,

$$\begin{aligned} \phi_{j+1} &= \phi_j + \frac{\omega_j}{\overline{\omega}}\psi_j \\ \psi_{j+1} &= -a_2\psi_j + \hat{a}_1\overline{\omega}\omega_j\cos\phi_{j+1} \end{aligned} \tag{15}$$

where $\hat{a}_1 = 2Aa_1/g$. We refer to (15) as the high-bounce map. We will find the fixed-point solutions of this high bounce map and use this to estimate the parameters of the BBA.

5.1 Determination of the co-efficient of restitution using periodic solutions to high-bounce map

The periodic solutions to the high-bounce map and the data collected for various 1-cycle periodic motions are used to compute the value of 'e'. The data needed for the frequency and the phase of the piston at bounce, is obtained from a stable 1-cycle periodic motion of the ball. These parameters are compared to the experimentally obtained parameters. This is a good indicator of the effectiveness of the periodic solutions of the nonlinear ball map to represent the actual experimental system for periodic motion of the ball.

For the m=1 case, we seek fixed points of the nonlinear ball map given by (15). The fixed points are required to satisfy the conditions $\phi_{j+1} = \phi_j$ and $\psi_{j+1} = \psi_j$. In order to obtain the fixed points, the right hand side of the first equation of (15) must be evaluated modulo 2π, in which case we obtain

$$\begin{aligned} \overline{\psi} &= 2n\pi \\ \overline{\phi} &= \arccos\left[\frac{2n\pi(1+a_2)}{\hat{a}_1\omega^2}\right] \end{aligned} \tag{16}$$

Expanding the values of a_2, $\hat{a}_1$ and rewriting (16) in terms of e we get,

$$e = \frac{\pi g(1+2M) - A\omega^2 \cos\overline{\phi}}{A\omega^2 \cos\overline{\phi} + \pi g} \tag{17}$$

The 'e' values in Table 2 are obtained from equation (17).

Frequency (rad/s)	Phase of piston at bounce - ϕ_j	Co-efficient of restitution – e
27	25.32°	0.8222
29	37.16°	0.8177
31	44.86°	0.8133
33	50.83°	0.8106
35	56.23°	0.8134

Table 2: The e values obtained by using the solutions to the nonlinear ball map, at different frequencies and the corresponding value of the phase of the piston at bounce

The mean value of e is found to be **0.815**, which is the very close to the value of 0.822 found using the stable 1-cycle periodic motion along with the definition of e.

5.2 Linear map as determined from high-bounce map

The linearization of the ball map in (15) gives

$$\begin{aligned} x_{1_{j+1}} &= x_{1_j} + x_{2_j} + b_1 u_j \\ x_{2_{j+1}} &= a_{21} x_{1_j} + a_{22} x_{2_j} + b_2 u_j \end{aligned} \tag{18}$$

where x_1, x_2, u represent the perturbations from the nominal values as given in (9.1) and (9.2), and $a_{21} = -\hat{a}_1\omega^2 \sin\overline{\phi}$, $a_{22} = -a_2 - \hat{a}_1\omega^2 \sin\overline{\phi}$, $b_1 = \frac{\overline{\psi}}{\overline{\omega}}$, $b_2 = a_{21}b_1 + \hat{a}_1\omega^2 \cos\overline{\phi}$

Substituting the parameters of the BBA we get,

$$A = \begin{bmatrix} 1 & 1 \\ -1.6457 & -0.9446 \end{bmatrix} \text{ and } b = \begin{bmatrix} 0.2094 \\ -0.2821 \end{bmatrix}$$

the eigenvalues of the A matrix are

λ = -0.02772±0.8369i ($|\lambda| = 0.837$)

6 Parameters of the BBA

The parameters of the BBA found using the two methods are summarized in Table 3.

a)

Mass of ball	23.3g
Mass of piston	348g
Mass ratio – M	0.066954
e	0.822
A	0.008m

b)

Mass of ball	23.3g
Mass of piston	348g
Mass ratio - M	0.066954
e	0.815
A	0.008m

Table 3: a) 'e' found using the definition and data collected from stable 1-cycle periodic motion of the ball b) 'e' found using experimental data and periodic solutions to high-bounce map.

The parameters of the high bounce map using the two parameters obtained from the two different methods are given in Table 4.

a)

a_1	1.7077
a_2	-0.7077
$\hat{a}_1$	0.00279

b)

a_1	1.701
a_2	-0.701
$\hat{a}_1$	0.00277

Table 4: a) Parameters computed using values in Table 3 a). b) Parameters found using values in Table 3 b)

The two sets of values in table 3 and table 4 are almost identical. Using the information in tables 3 b) and 4 b) to examine the eigenvalues of the linearized ball map in (18), we obtain information regarding the stable periodic motion, which is summarized in the following two tables, Table 5 and Table 6. Similar tables were constructed using the parameters in table 3 a) and table 3 b) and the values were found to be almost similar to the ones obtained before.

Table 5: Minimum value of ϖ for which a stable period-1 (m=1) solution exists with the corresponding phase angle ϕ and bounce height

n	Frequency (rad/s)	Phase (in degrees)	Height (m)
1	25.7	3.15	0.0733
2	36.4	5.45	0.1461
3	44.5	2.44	0.2200
4	51.4	3.16	0.2932
5	57.5	4.18	0.3661
6	63.0	4.47	0.4391

Table 6: Maximum value of ϖ for which a stable period-1 (m=1) solution exists with the corresponding phase angle ϕ and bounce height

n	Frequency (rad/s)	Phase (in degrees)	Height (m)
1	37.3	61.7	0.0348
2	42.4	42.81	0.1077
3	48.2	31.62	0.1875
4	53.9	24.77	0.2666
5	59.3	20.33	0.3442
6	64.3	16.85	0.4215

We use this table as a starting point to pick a frequency to produce chaotic motion in our next section where we design a chaotic controller to control the ball to stable period-1 orbit starting from rest. From the table, it is evident that the following frequencies will not support m=1 periodic motion.

$$42.4 < \omega < 44.5$$
$$48.2 < \omega < 51.4$$
$$53.9 < \omega < 57.5$$

We will pick a frequency of 44 rad/s to produce the chaotic motion or a chaotic transient to a periodic motion with m>1. This is used to get into the region of domain of attraction to the specified periodic solution.

7 Controlling the ball to 1-cycle stable periodic orbits

From the previous analysis, it is evident that the high-bounce map is a fairly good representation of the BBA. A combination of the linear map about the stable orbit and the high-bounce map is needed to estimate the domain of attraction to stable 1-cycle periodic orbits. We use the two different linear maps obtained earlier to design the controllers to put the ball into the 1-cycle stable periodic orbits starting from rest on the plate. The efficiency of the controllers in putting the ball into the domain of attraction and

keeping it there is dependent on the accuracy of the estimate of the domain of attraction. This is dependent on the accuracy of the linear maps used to represent the BBA. Data collected directly from the BBA is used to evaluate the efficiency of the controllers. This is then used to determine as to which of the linear maps is a more accurate representation of the BBA.

7.1 Domain of attraction from experimental data

Chaos is created using open loop control of the piston using a sinusoidal input and this is used to take the ball into the domain of attraction [5]. The key feature in this algorithm is to be able to estimate the domain of attraction accurately.

Using the linear map obtained from the experimental data,

$$A = \begin{bmatrix} -0.5708 & 0.5111 \\ -1.6194 & 0.5201 \end{bmatrix},$$

with eigenvalues of λ = -0.0254±0.7281i ($|\lambda| = 0.729$) lying inside the unit circle. Thus, there must exist a 2x2 symmetric positive definite solution for P satisfying the discrete Lyapunov equation

$$A^T PA - P = -Q\,,$$

where Q is any 2x2 symmetric positive definite matrix such that

$$V = X^T PX$$

is a Lyapunov function for the bouncing ball system. Choosing $Q = I$, we obtain

$$P = \begin{bmatrix} 5.474 & -1.6077 \\ -1.6077 & 2.1593 \end{bmatrix}$$

The control algorithm used is the chaotic control algorithm as described in [5]. The ball is initially driven with at a frequency that will produce chaotic motion or a chaotic transient to a periodic motion. This frequency was chosen to be 44 rad/s using the periodic frequency table. When the ball enters the domain of attraction to the stable 1-cycle periodic orbit at 30 rad/s, the driving frequency is changed to the stable 30 rad/s. The key step is to identify whether the ball has entered the domain of attraction. This can be done by solving an optimization problem of finding the largest $V(x) < V_{\max}$ for which ΔV or $\dot{V}$ is negative [8]. For two-dimensional systems, this can be simplified by choosing a value of $V_{\max}$, set up differential equations for evaluating around the level curve $V(x) = V_{\max}$ and then calculating $\dot{V}$ at every integration step. We repeat this by choosing higher values of $V_{\max}$ until $\dot{V}$ does not remain negative at every point. Thus we can pick the highest value for which $\dot{V}$ remains negative at every point to represent the domain of attraction for the system. Using this procedure, we obtain

for $\omega = 30 rad/s$, $V_{\max}$ = 1.25.

The chaotic control algorithm is now used to control the ball to periodic orbits, starting from rest on the piston, in the bouncing ball experiment. Figure 9 shows the data collected directly from the experiment. The dotted line indicates the path of the ball and the circle indicates the state of the ball at the time of bounce. The solid elliptical line indicates the boundary of the domain of attraction corresponding to the stable orbit for $\omega = 30 rad/s$, which was estimated using the linear map obtained from experimental data.

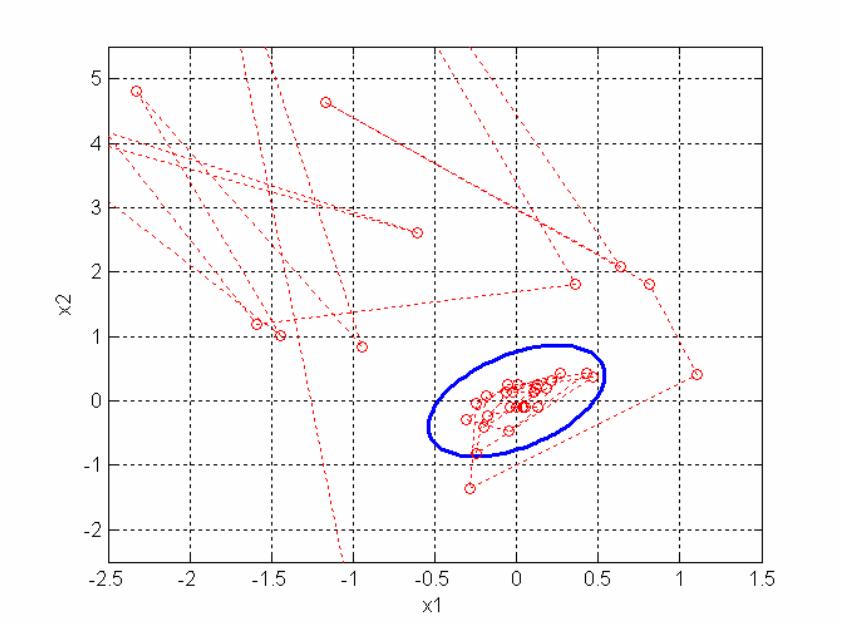

Figure 9: Plot of the ball driven chaotically in state space before being capture within domain of attraction estimated using the linear map obtained from experimental data.

Another run of the experiment is carried out to find out if the ball remains in a stable periodic orbit, once it is captured within the domain of attraction. Figure 10 shows the ball after it has been captured within the domain of attraction and is undergoing a number of 1-cycle periodic bounces. It is observed that the ball is in a stable motion. Figure 11 shows that the corresponding bounce heights are almost equal and constant to the stable bounce height indicated by the dashed line in the figure.

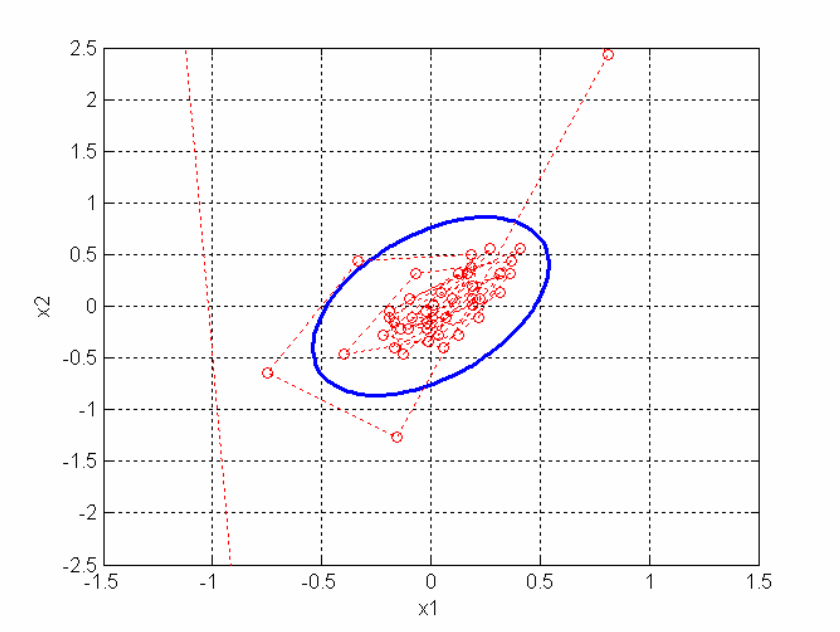

Figure 10: Plot of motion of ball within domain of attraction showing number of stable periodic 1-cycle bounces

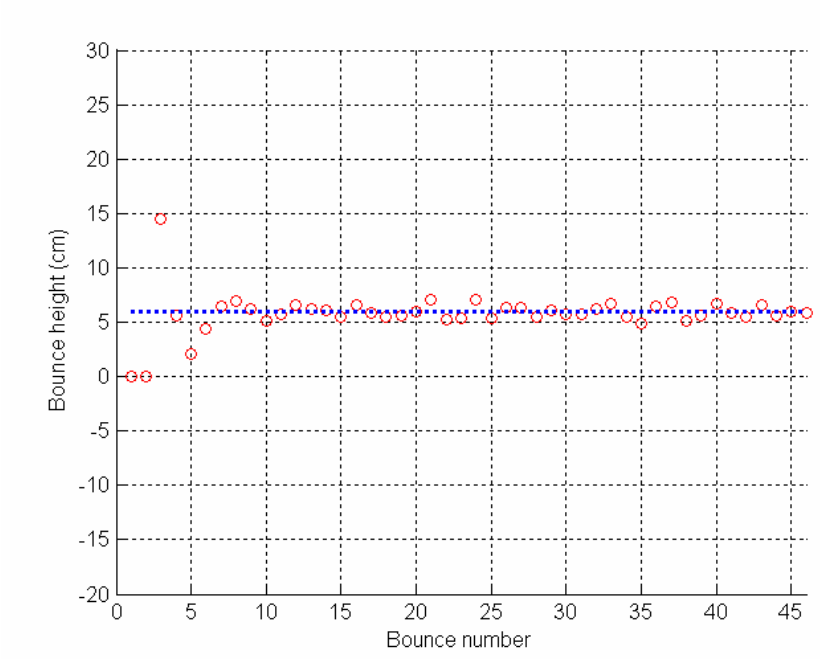

Figure 11: A number of stable 1-cycle periodic bounce heights within the domain of attraction

7.2 Domain of attraction from high-bounce map

The linear map obtained by linearization of the high-bounce map is now used to estimate the domain of attraction. Using this we get,

$$A = \begin{bmatrix} 1 & 1 \\ -1.6457 & -0.9446 \end{bmatrix}.$$

The chaotic frequency of 44 rad/s and the stable 1-cycle periodic frequency of 30 rad/s chosen for the earlier approach is found to work here. Following the same procedure described earlier, the P matrix is obtained as

$$P = \begin{bmatrix} 9.1787 & 5.0583 \\ 5.0583 & 5.7782 \end{bmatrix}$$

and the boundary of the domain of attraction is defined by,

$$V_{\max} = 8, \text{ for } \omega = 30 rad/s,$$

These parameters are used in the controller for the bouncing ball system. The ball is started from rest on the piston as before and the chaotic control algorithm is used to control the ball to a periodic orbit. The data collected directly from the experiment is plotted in Figure 12. The solid elliptical region represents the domain of attraction estimated using the linearized high-bounce map. The dashed elliptical region indicates the domain of attraction obtained directly from the experimental data. It is seen that the domain of attraction estimated using the linear map from the direct experimental method is in a different direction and is much smaller than the one estimated from the linearized ball map.

The ball is driven chaotically in state space before being captured within the domain of attraction and driven to the fixed point. It is observed on the plot that the ball enters the domain of attraction indicated by the solid line a number of times but is not captured. The periodic bounces of the ball about the stable orbit clearly shows that the linear map from the experimental data gives a better estimate for the domain of attraction.

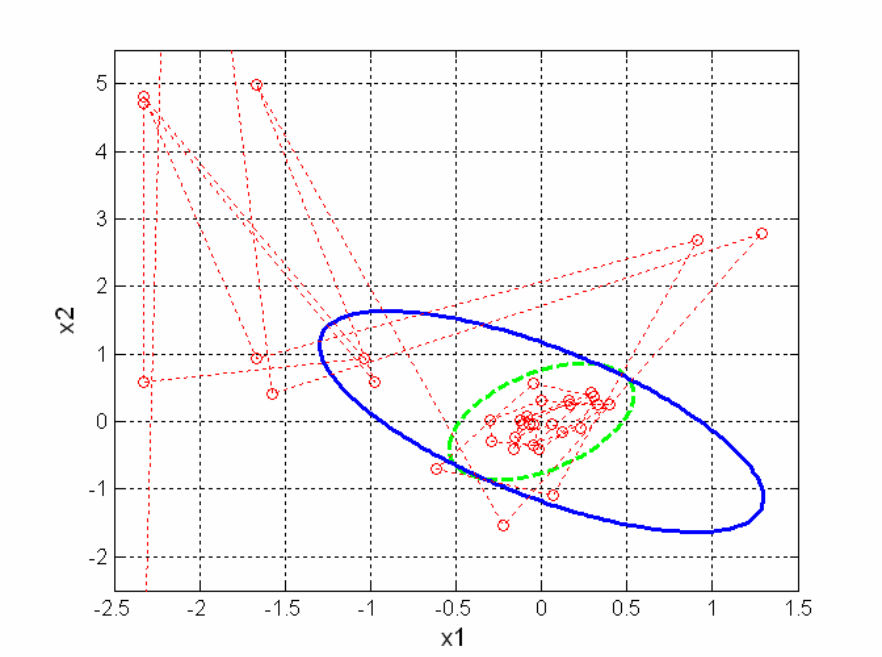

Figure 12: Plot of the ball driven chaotically in state space with domain of attraction obtained using linear map obtained from the linearization of the high-bounce map

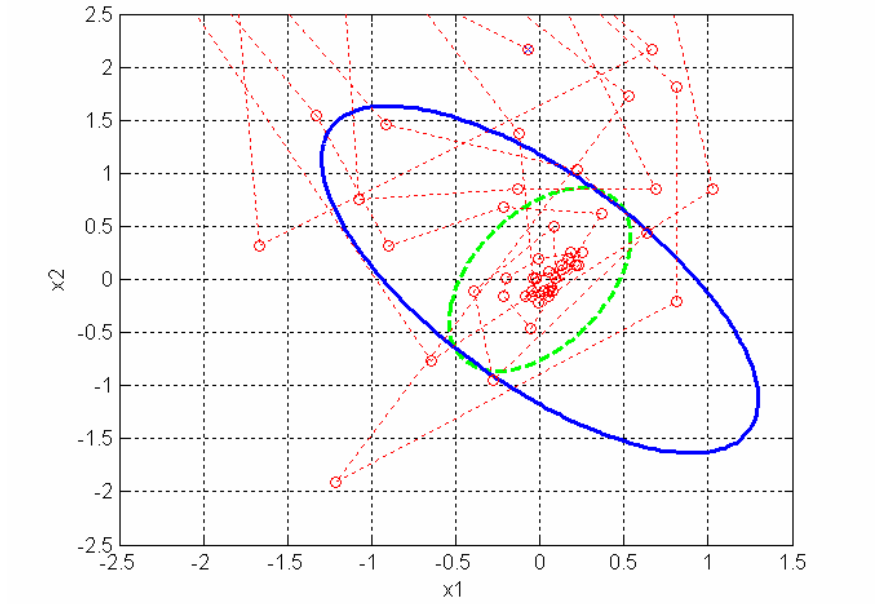

Figure 13: Data collected after the ball had entered the domain of attraction – ball is seen to leave the domain of attraction and return to the fixed point a few times.

Figure 13, show that even though the ball enters the domain of attraction, reaches the stable orbit and executes a number of stable 1-cycle periodic bounces it has a tendency to leave the domain of attraction. The chaotic control will ultimately bring the ball back to the stable orbit but this shows that the estimate of the domain of attraction obtained using the linearized high-bounce map is not accurate.

8 Conclusions

The linear map from experimental data gives a more accurate estimate of the domain of attraction and hence produces a more effective controller. The controller using the estimate of the domain of attraction from the linearized high-bounce map is ineffective but is found to work. This is because the linearized high-bounce map gives a much larger estimate for the domain of attraction and it completely encloses the estimate of the domain of attraction obtained from the experimental data based linear map. The ball tends to leave the domain of attraction as estimated from the linearize ball map, and is driven chaotically in state space according to the chaotic control algorithm. Ultimately, the controller puts it back into a stable orbit and this cycle continues. The algorithm is robust enough to tolerate inaccuracies in the estimate of the domain of attraction, so as to be able to put the ball back into the stable orbit. But, it desirable to have the ball maintain a stable periodic orbit once it enters the domain of attraction as in the case when the domain of attraction estimate is obtained from the experimental data based linear map.

These results can be extended to the case of designing a controller to one of the unstable periodic orbits. This requires the design of a linear controller to drive the ball to the stable orbit once it enters the domain of attraction. Generally, a linear controller is designed using a linear map of the system about the fixed point. This requires an accurate estimate of the linear map of the system about the fixed point. In order to obtain an accurate linear map for the highly nonlinear bouncing ball apparatus, the data based experimental approach is preferred to the linear map obtained by linearization of the high-bounce map. As approximations were made to simplify the high-bounce map, it does not yield an accurate map on linearization.

It was found that conventional methods could not be used to determine the value of the coefficient of restitution (e), an extremely sensitive parameter of the system. Using the stable 1-cycle periodic orbits to determine the value of ‘e’ provided insights into how the we can take advantage of the system dynamics to determine its value accurately. The accurate determination of ‘e’ also allowed us to predict the frequencies at which periodic and chaotic motion occurs for the apparatus, thereby allowing us to use the chaotic control algorithm effectively for control of the ball.

It is quite evident that the bouncing ball system from Launch Point Technologies provides an excellent experimental tool to study nonlinear dynamics and chaos. The apparatus can be used to study the variety of chaotic or periodic motions possible, depending on the initial conditions of the ball and the piston. Improved modeling techniques cane be used to obtain a better model of the system. Various conventional control algorithms can be applied to study their effectiveness for this highly nonlinear, yet simple mechanical system.

References

[1] Guckenheimer, J. and Holmes, P., 1993, *Nonlinear Oscillations, Dynamical Systems and Bifurcations of Vector Fields*, Springer-Verlag, NY.

[2] Vincent, T. L., 1995, “Controlling a ball to bounce at a fixed height”, *Proceedings of the 1995 American Control Conference*, Seattle, WAS, June, pp. 842-846.

[3] Vincent, T. L., and Mees, A. I., 1999, “Controlling a bouncing ball”, *Int. J. Bifurcation and Chaos*, **10**, No. 3, pp. 579-592.

[4] Mintah, B., 2001, “Data based linear approximation method to the chaotic control of a bouncing ball”, *Masters of Science Thesis*, Department of Aerospace and Mechanical Engineering, University of Arizona.

[5] Vincent, T. L., 1997, “ Control using chaos”, IEEE Contr. Syst., **17**, No. 6, pp. 65-76.

[6] Ghosh, J. and Paden, B., 1999, “Control of 2-periodic motion for bouncing ball”, *Proceedings of the 1999 American Control Conference*, San Diego, CA, June, pp. 4048-4050.

[7] Ogata, K., 2000, *Modern Control Engineering*, Prentice Hall, 3rd edition, June.

[8] Grantham, W. J. and Vincent, T. L., 1993, *Modern Control Systems: Analysis and Design*, John Wiley and Sons, Inc.

[9] Stensgaard, I., and Laegsgaard, E., 2001, “Listening to the coefficient of restitution – revisited”, *Am. J. of Phys.*, **69**, No. 3, March, pp. 301 –305.